Journal of Cellular Biochemistry 95:794–804 (2005)

XRCC1 and DNA Polymerase β Interaction Contributes to Cellular Alkylating-Agent Resistance and Single-Strand Break Repair

Heng-Kuan Wong and David M. Wilson III*

Laboratory of Molecular Gerontology, National Institute on Aging, 5600 Nathan Shock Drive, Baltimore, Maryland 21224

Abstract X-ray cross complementing 1 (XRCC1) protein has been suggested to bind to DNA single-strand breaks (SSBs) and organize protein interactions that facilitate efficient DNA repair. Using four site-specifically modified human XRCC1 mutant expression systems and functional complementation assays in Chinese hamster ovary (CHO) XRCC1-deficient EM9 cells, we evaluated the cellular contributions of XRCC1s proposed N-terminal domain (NTD) DNA binding and DNA polymerase β (POLβ) interaction activities. Results within demonstrate that the interaction with POLβ is biologically important for alkylating agent resistance and SSB repair, whereas the proposed DNA binding function is not critical to these phenotypes. Our data favor a model where the interaction of XRCC1 with POLβ contributes to efficient DNA repair in vivo, whereas its interactions with target DNA is biologically less relevant. J. Cell. Biochem. 95: 794–804, 2005. Published 2005 Wiley-Liss, Inc.†

Key words: XRCC1; POLβ; DNA binding; EM9; functional complementation; base excision; single-strand break repair

Single-strand breaks (SSBs) are common products formed in the genome, either by free radical attack or nuclease-catalyzed strand cleavage of the phosphodiester backbone [Lindahl, 1993; Nishino and Morikawa, 2002]. If unrepaired, these DNA products can promote genetic instability, mainly because a SSB can become a recombinogenic double strand break upon DNA replication fork collapse [Helleday, 2003]. Most of the SSB damage is removed by components of the related base excision repair (BER) and single-strand break repair (SSBR) pathways [Caldecott, 2003; Wilson et al., 2003]. X-ray cross-complementing 1 (XRCC1) is a major contributor to the repair of SSBs in DNA, likely by facilitating specific protein–protein interactions during the process [Thompson and West, 2000; Caldecott, 2003]. These interactions are mediated primarily through three functional domains in XRCC1: its N-terminal domain (NTD), and its two BRCA1 carboxyl-terminal (BRCT) modules, denoted BRCT-1 and BRCT-2.

BRCT-1, located near the center of the XRCC1 protein, is critical for cell survival following treatment with methyl methanesulfonate (MMS) and efficient SSBR during both G_1 and S/G_2 cell-cycle phases [Taylor et al., 2002; Kubota and Horiuchi, 2003]. This region directs interactions with PARP-1 and -2—two key nick sensor proteins—such that XRCC1 negatively regulates their poly (ADP-ribose) polymerase activities, while being a polymer acceptor of both enzymes itself [Masson et al., 1998; Schreiber et al., 2002]. El Khamisy et al. [2003] demonstrated that mutation of the BRCT-1 domain reduces the appearance of XRCC1 foci in hamster cells following H_2O_2 treatment, suggesting that PARP-1 is required for the assembly of XRCC1 at sites of strand breaks upon oxidative damage. In addition, these authors failed to detect nuclear XRCC1 foci after H_2O_2 treatment in mouse cells harboring a targeted disruption of the *Adprt1* gene, which encodes PARP-1.

The C-terminal BRCT-2 domain of XRCC1 interacts with DNA ligase 3α (Lig3α), a protein that functions to seal the final repair nick

*Correspondence to: David M. Wilson III, Laboratory of Molecular Gerontology, National Institute on Aging, 5600 Nathan Shock Drive, Baltimore, Maryland 21224.
E-mail: wilsonda@grc.nia.nih.gov

Received 22 December 2004; Accepted 28 January 2005
DOI 10.1002/jcb.20448

intermediate [Caldecott et al., 1994; Nash et al., 1997]. These proteins bind to each other through their respective C-terminal BRCT domains to form a stable heterodimer [Nash et al., 1997], and the interaction is critical for stabilizing the Lig3α protein in vivo [Caldecott et al., 1994]. Taylor et al. [2000] described a cell-cycle-dependent role for BRCT-2, concluding that the XRCC1–DNA Lig3α complex is essential for DNA strand break repair in G_1. In fact, the BRCT-2 domain appears necessary for preserving genetic stability in postmitotic tissues in vivo [Moore et al., 2000]. Data from Kubota and Horiuchi [2003] showed that the BRCT-2 motif contributes to fast SSBR, as XRCC1 BRCT-2-defective cells display a reduced repair rate in vivo.

The NTD of XRCC1 has been shown to interact with DNA polymerase β (POLβ) in vitro [Kubota et al., 1996; Marintchev et al., 2003]. POLβ is the major gap-filling DNA polymerase and exhibits dRP lyase activity for hydrolytic and C-4′ oxidized 5′-abasic residues in BER [Wilson, 1998; Demple and DeMott, 2002]. The interaction between XRCC1 and POLβ occurs in the palm-thumb domains of POLβ [Gryk et al., 2002]. Furthermore, XRCC1-NTD has been shown to interact with DNA containing a single-strand nick or gap [Marintchev et al., 1999, 2000]. The combination of structural and biochemical mapping studies suggests a potential mechanism for the cooperative interaction of XRCC1-NTD and POLβ on gap DNA substrates [Marintchev et al., 1999; Gryk et al., 2002]. Recently, Marintchev et al. [2003] showed the importance of specific amino acid residues within the β-strands D and E of the five-stranded β-sheet and the α2 helix of XRCC1-NTD in POLβ binding using site-directed mutagenesis.

Four Chinese hamster ovary (CHO) cell lines with XRCC1 mutations have been characterized (EM7, EM9, EM-C11, and EM-C12) [Shen et al., 1998]. Most studies have utilized EM9, and these cells have been shown to exhibit reduced Lig3 expression [Ljungquist et al., 1994], SSB processing [Whitehouse et al., 2001], and abasic endonuclease activities [Vidal et al., 2001]. This and other cell lines deficient in XRCC1 are extremely hypersensitive to alkylating agents (~10-fold), such as ethyl methanesulfonate (EMS) and MMS [Thompson et al., 1982], show moderate sensitivity to H_2O_2 [Cantoni et al., 1987] and camptothecin (two–fivefold) [Barrows et al., 1998], and weak (<twofold) or no sensitivity to ionizing radiation [Thompson et al., 1990], *N*-ethyl-nitrosourea, *N*-methyl-*N*-nitro-*N*-nitrosoguanidine, mitomycin C, ultraviolet C radiation, ultraviolet A radiation, and heavy metals (reviewed in [Thompson and West, 2000; Caldecott, 2003]). XRCC1 mutant CHO cells also exhibit a defect in rejoining chromosomal SSBs following EMS or MMS treatment, relative to wild-type controls. In addition, EM9 cells display increased frequencies of sister chromatid exchange (SCE), chromosomal aberrations, and genetic deletions. XRCC1-knockout mice are embryonic lethal [Tebbs et al., 1999], indicating an essential role for this protein in embryogenesis.

Collective evidence indicates that XRCC1 acts as a scaffold protein, recruiting and presumably facilitating the enzymatic activities of several BER/SSBR participants. Besides the interactions described above, XRCC1 also associates with the following replication/repair proteins: proliferating cell nuclear antigen (PCNA) [Fan et al., 2004], polynucleotide kinase (PNK) [Whitehouse et al., 2001], tyrosyl DNA phosphodiesterase (TDP1) [Plo et al., 2003], Aprataxin [Gueven et al., 2004; Sano et al., 2004], 8-oxoguanine DNA glycosylase (OGG1) [Marsin et al., 2003], and apurinic endonuclease (APE1) [Vidal et al., 2001]. We set out here to evaluate the biological significance of the reported XRCC1–POLβ interaction, as well as the proposed DNA binding activity of XRCC1, using site-specific XRCC1 mutants and functional complementation assays in EM9 cells.

MATERIALS AND METHODS

Reagents and Cell Lines

All oligonucleotides were purchased from Midland Certified Reagent Company (Midland, TX). The CHO wild-type AA8 and XRCC1 mutant EM9 cell lines were a gracious gift of Dr. Larry H. Thompson (Lawrence Livermore National Laboratory).

Mammalian XRCC1 Expression Systems

To generate the wild-type pcDNA3–XRCC1 expression system, the human XRCC1 cDNA was amplified using the following oligonucleotide primers: X15′Eco, 5′-CGGAATTCACCATGCCGGAGATCCGCCTCCG-3′ and X13′Xba, 5′-GCTCTAGATCAGGCTTGCGGCACCACCC-3′. The resulting PCR product was then digested

with EcoRI and XbaI restriction enzymes and subcloned into the corresponding sites within pcDNA3 (Invitrogen, Carlsbad, CA). Recombinant plasmids were verified by restriction digestion and complete sequence analysis (performed by Lark Technologies, Inc., Houston, TX). The XRCC1 site-specific mutant plasmids (F67A, E69K, V86R, and R109A) were created using an overlapping PCR mutagenesis technique. In brief, two XRCC1 PCR products were generated. PCR Prod1 was produced using primers X1MutA (5′-GCAGCCAAGGCAGGCGAGAA-3′) and X1Eco47III (5′-ACCCGGTCCCAGCGCTTCTCGGCGGC-3′), and the mutant-containing product, Prod2, was generated using X15′Eco and one of the following primers (the location of the altered codon is indicated by the underline): X1F67A (5′-CAGCACCTCCACGGCAGCTGAGCCATCA-3′), X1E69K (5′-CCCACCAGCACCTTCACGAAAGCTGAG-3′), X1V86R (5′-GTGACCAGAAGGCGCTCATAGTCTTG-3′), or X1R109A (5′-GGCCCAAACATGGCAACGCGGTTGGG-3′). Next, Prod1 and Prod2 were mixed at a 1:10 ratio, and Prod3 was generated by amplification with X15′Eco and X1Eco47III. This third PCR product was then digested with EcoRI and Eco47III (Fermentas, Hanover, MD) and subcloned into the same sites within the *XRCC1* coding region of pcDNA3–XRCC1. The replaced ~400 nt *XRCC1* fragment was sequenced by Lark Technologies, Inc.

Stable XRCC1-Expressing EM9 Cell Lines

A wild-type or site-specific mutant pcDNA3 plasmid (see above) was purified using a Qiagen kit (Valencia, CA) and transfected into the CHO EM9 cell line by electroporation using Nucleofactor solution T from Amaxa Biosystems (Gaithersburg, MD). Cell lines harboring pcDNA3 recombinant plasmid(s) were then selected with 600 μg/ml geneticin (G418, Gibco, Invitrogen). Human XRCC1 protein expression was analyzed using standard Western blot techniques. In brief, roughly 2 million cells were harvested and resuspended in SDS loading buffer or RIPA buffer (1× PBS, 1% Nonidet P-40, 0.5% sodium deoxycholate, 0.1% SDS, 0.5 mM phenylmethylsulfonyl fluoride, and complete protease inhibitor (Roche Molecular Biochemicals, Indianapolis, IN)). Protein concentrations were determined by the Bio-Rad protein assay (Hercules, CA) and confirmed by standard 10% SDS–polyacrylamide gel electrophoreosis and coomassie blue staining. For Western blotting, following electrophoresis, proteins were transferred to a PVDF membrane and probed with antibody against the human XRCC1 protein (clone 33-2-5 from Neomarkers, Fremont, CA), Lig3α (BD Biosciences, San Jose, CA), or POLβ (Trevigen, Gaithersburg, MD). Visualization was performed using the ECL Plus system (Amersham Pharmacia, Piscataway, NJ) or the SuperSignal West Femto maximum sensitivity kit (Pierce, Rockford, IL).

MMS Sensitivity Analysis

EM9 complemented (with wild-type or mutant XRCC1), EM9 vector, and parental AA8 cells were cultured in DMEM (Gibco, Invitrogen) plus 10% fetal bovine serum, 1% glutamine, and 1% penicillin-streptomycin. To investigate MMS sensitivity, colony forming assays were performed. Briefly, 3×10^2 cells were plated onto a 60 mm dish, incubated for 16 h, and then treated with different concentrations of MMS for 1 h. The cells were washed with phosphate-buffered saline (PBS) twice and incubated for 7–10 days with fresh medium to allow colony formation. Resulting colonies were stained with methylene blue and counted. The surviving fraction was calculated by dividing the number of colonies in treated dishes by those counted in untreated control dishes. The cytotoxicity of MMS was also determined using the differential cytotoxicity (DC) assay, which is a modified colony forming assay [Hoy et al., 1984].

Intracellular NAD(P)H Level Measurement

This method is based on the reduction of water soluble 2-(2-methoxy-4-nitrophenyl)-3-(4-nitrophenyl)-5-(2,4-disulfophenyl)-2H-tetrazolium monosodium salt (CCK-8) to a yellow colored formazan dye by dehydrogenases [Nakamura et al., 2003]. The amount of the formazan dye is directly proportional to the number of living cells. In brief, cells were seeded in 96-well plates (5×10^3 cells) as described above in normal medium and incubated for 16 h. After 1 h treatment with different concentrations of MMS, the cells were washed with PBS, and 100 μl of medium and 10 μl of CCK-8 solution (Dojindo Molecular Technology, Gaithersburg, MD) were added to each well. Cells were cultured for up to 4 h, and the amount of formazan dye produced by living cells was measured using a spectrophotometer at 450 nm.

Comet Assay

Cells were treated with MMS (0.6 mM) for 10 min and incubated with fresh medium for 0, 30, or 240 min to allow repair. Once harvested, cells were analyzed as described [Speit and Hartmann, 1999]. Cell suspensions (20,000 cells) in 1.2% low melting point (LMP) agarose dissolved in PBS were spread onto microscope slides precoated with 1% normal melting point (NMP) agarose. The cells were then lysed overnight at 4°C in 2.5 M NaCl, 100 mM EDTA, 10 mM Tris, pH 10, 10% sodium lauroyl sarcosinate, 10% DMSO, and 1% Triton X-100. After lysis, the slides were placed in an electrophoresis unit and DNA was allowed to unwind for 30 min in the electrophoresis solution of 300 mM NaOH and 1 mM EDTA, pH > 13. Electrophoresis was conducted at 4°C for 30 min at 30 V (300 mA). The slides were then washed three times with neutralization buffer (0.4M Tris, pH 7.5), stained with 5 μg/ml ethidium bromide, and covered with cover slips. The slides were placed at 4°C in a humidified air-tight container prior to analysis. Comets were visualized using an epifluorescence microscope (Zeiss, Germany) connected to a Zeiss camera. Komet 5.5 software developed by Kinetic Imaging (Liverpool, UK) was used to analyze 100 cells per slide. The tail moment, defined as the product of the DNA in the tail and the tail length was used to quantitate DNA breaks.

RESULTS

Wild-Type XRCC1-Expressing EM9 Cell Lines

We first created a stable wild-type human XRCC1 expressing EM9 cell line. EM9 cells are XRCC1-deficient due to a C–T nucleotide substitution within the *XRCC1* coding region [Shen et al., 1998]. This mutation introduces a stop codon at nucleotide 661 of the open reading frame, resulting in a truncated polypeptide of 220 residues that is unstable. Nine independent geneticin-resistant EM9 clones, which had stably integrated the wild-type human XRCC1 pcDNA3 plasmid, were examined for protein expression. Three of these were found to express human XRCC1 at low (clone 7; seen upon longer exposure, not shown), moderate (clone 3), or high (clone 8) levels (Fig. 1A). The human XRCC1 positive clones were then tested for MMS resistance relative to EM9 and the AA8 cell line using a qualitative DC assay (see "Materials and Methods"). Consistent with the level of human XRCC1 protein expression, clone 8 exhibited the highest degree of resistance, followed by clone 3 and clone 7, with all isolates displaying greater resistance to MMS than the XRCC1-deficient EM9 cells (Fig. 1B). Clone 8 (EM9-WT) exhibited a similar MMS sensitivity profile to that of the AA8 line and was used in subsequent comparative analysis.

Establishment of XRCC1 Mutant-Complemented EM9 Lines

The major functional (interactive) domains of XRCC1 are depicted in Figure 2A and are described in detail in the introduction. We created four site-specific mutations within the XRCC1-NTD coding region (Fig. 2A) to disrupt either the POLβ-interaction (E69K and V86R), the DNA binding (R109A), or both activities simultaneously (F67A). This mutagenesis was directed by previous high-resolution NMR studies and biochemical analyses, which detailed the role of these residues in mediating XRCC1 protein–protein and/or protein–DNA interactions [Gryk et al., 2002; Marintchev et al., 2003]. We elected to scrutinize four XRCC1 mutant proteins, as we felt this would add needed redundancy to slight variations that might occur in generating or characterizing complemented cell lines.

We next established stably-transfected EM9 cell lines that expressed each of the four XRCC1 mutants at levels similar to that observed in EM9-WT (Fig. 2B, top panel). A densitometry scan was performed to determine the comparative protein levels, and these values are shown under each representative lane. The various complemented lines were also examined for endogenous levels of POLβ and Lig3. Western blot analysis of whole cell extracts revealed that POLβ was present at similar (or higher) levels in each of the lines (Fig. 2B middle-panel). A pcDNA3 vector-complemented EM9 cell line (EM9-V) was found to possess levels of POLβ equivalent to, but levels of Lig3 ~fivefold lower than, EM9-WT, an observation consistent with previous reports [Caldecott et al., 1995]. Significantly, while Lig3 protein expression was found to be comparable in most of the mutant-complemented cell lines relative to EM9-WT (Fig. 2B, bottom panel), and generally mimicked the XRCC1 level, Lig3 was consistently found to be at a lower concentration (~twofold) in EM9-V86R. These lines (Fig. 2B) were next

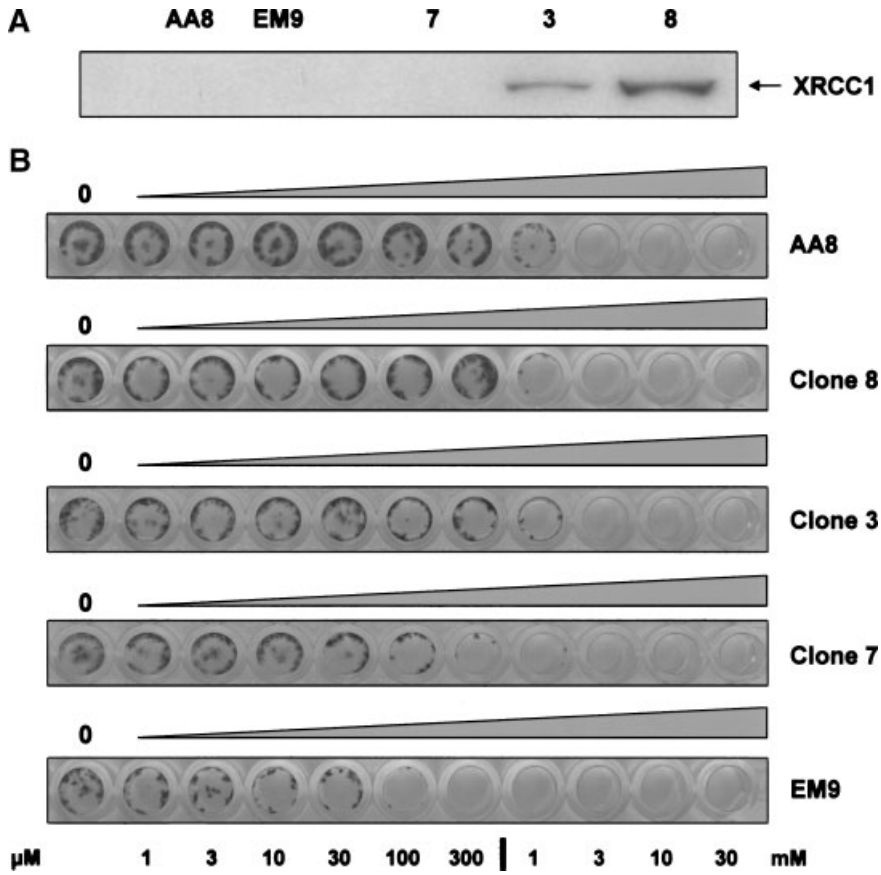

Fig. 1. Wild-type X-ray cross complementing (XRCC1) complemented EM9 cell lines and methyl methanesulfonate (MMS) sensitivity. **A**: Expression of wild-type human XRCC1 protein in EM9 isolates. Whole cell extracts from indicated cells were fractionated by SDS–PAGE, transferred to a PVDF membrane, and immunoblotted with anti-XRCC1 antibody. Three clones express human XRCC1 at low (clone 7), moderate (clone 3), and high (clone 8) levels as seen in this representative Western blot. The antibody used here does not cross-react with the endogenous Chinese hamster ovary (CHO) XRCC1 protein of AA8 cells. **B**: MMS resistance of XRCC1-complemented EM9 lines. Briefly, 3×10^4 cells were plate in a 96-well plate, incubated overnight, and then treated with 0, 1, 3, 10, 30, 100, 300 μM, 1, 3, 10, or 30 mM MMS (from left to right, indicated below images) for 1h. After 7–10 days in drug-free medium, plates were stained with methylene blue, which identifies living cells. A representative DC assay of three independent experiments is shown.

examined for their comparative resistance to MMS challenges.

Functional Complementation Capacity of XRCC1 Site-Specific Mutants

As shown in Figure 3A (EM9-WT), expression of wild-type XRCC1 restored MMS resistance essentially to the levels seen with AA8. Conversely, the EM9-V cell line exhibited no survival at any of the MMS concentrations tested (this is identical to what was seen with EM9 (no vector), data not shown). Notably, the three mutant XRCC1 clones that disrupted either the POLβ interaction exclusively (E69K and V86R) or both the POLβ and DNA binding functions of XRCC1 (F67A) displayed incomplete, albeit significant, phenotypic correction, with the EM9-V86R isolate demonstrating the worst complementation effectiveness (Fig. 3A). EM9 cells transfected with the XRCC1 R109A mutant, which was designed to be defective in the DNA binding function of the XRCC1-NTD, displayed a MMS resistance profile similar to AA8 and EM9-WT. The IC_{50} value (i.e., the concentration of MMS at which 50% cell killing is observed) for each of the cell lines is as follows: AA8 = 0.9 mM; EM9-WT and R109A = 0.8 mM; E69K and F67A = 0.34 mM; V86R = 0.14 mM; and EM9 < 0.1 mM (previously found to be 0.05 mM by El Khamisy et al. [2003]). In other words, E69K- or F67A-, and the V86R-complemented cells exhibited a 2.4-fold and a 5.7-fold higher sensitivity (i.e., lower IC_{50}), respectively, to MMS challenges than EM9-WT.

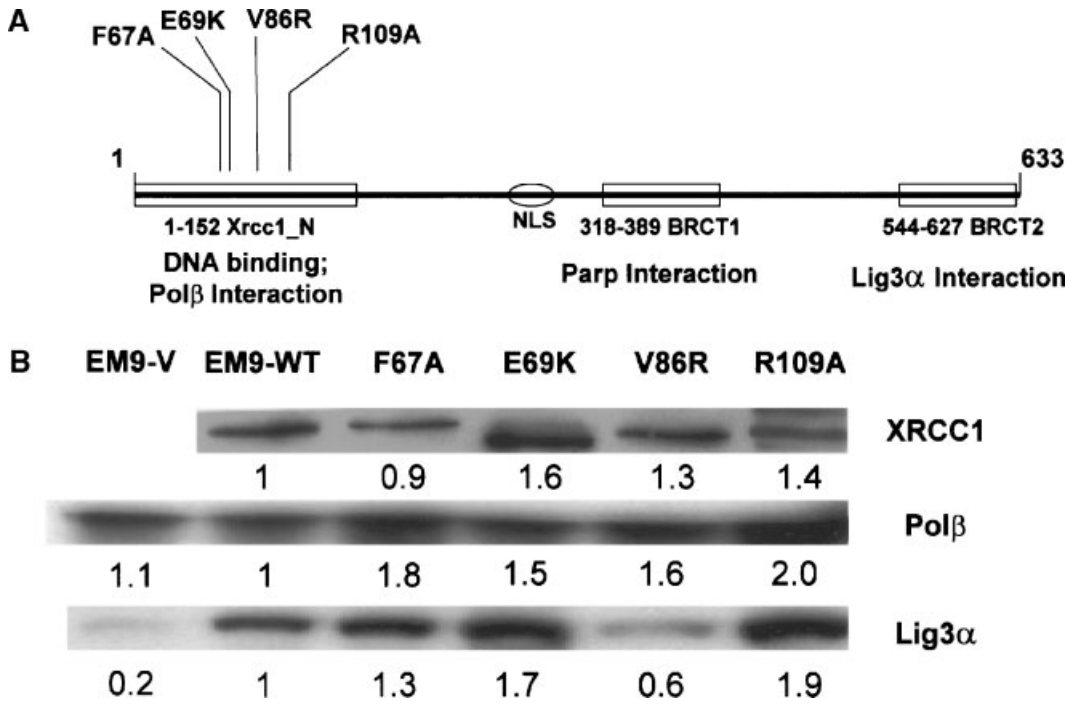

Fig. 2. Schematic of the XRCC1 protein and site-specific mutant XRCC1-complemented EM9 cell lines. **A**: XRCC1 protein schematic. XRCC1 (633 amino acids) contains an N-terminal domain (N-terminal domain (NTD) or Xrcc1_N), several putative nuclear localization signals (NLS), and two BRCA1 carboxyl-terminal (BRCT) modules, denoted BRCT-1 and BRCT-2. These different domains interact with several proteins (some indicated) as described in the Introduction. Site-specific mutations (shown) were generated in the DNA polymerase β (POLβ) interaction and/or DNA binding NTD (see text for details). **B**: Expression of wild-type (WT) and mutant XRCC1 proteins, as well as DNA ligase 3α (Lig3α) and POLβ. Whole cell extracts (20 μg total protein) from the different stable cell lines (indicated) were fractionated by SDS–PAGE, transferred to PVDF membrane, and immunoblotted with anti-XRCC1 antibody, anti-Lig3, or anti-POLβ (see Materials and Methods for details). Western blot data shown represents the typical results and trends of at least three independent experiments.

To further evaluate the complementation efficiency of the various XRCC1 mutants, we utilized a qualitative assay that measures intracellular NAD(P)H levels as a means of indirectly assessing SSBR in living cells [Nakamura et al., 2003]. Accumulation of strand breaks activates PARP-1 which catalyzes the formation of poly(ADP-ribose) polymers, resulting in NAD+ depletion [de Murcia and Menissier, 1994; Lindahl et al., 1995]. Thus, low intracellular NAD(P)H levels correspond to persistent PARP-1 activation and poor SSBR. As expected, EM9 cells harboring the pcDNA3 vector exhibited the lowest level of measured NAD(P)H at each MMS concentration (Fig. 3B). Conversely, EM9-WT cells exhibited the highest level of NAD(P)H, indicative of efficient SSB removal. Consistent with the survival data of Figure 3A, the NAD(P)H assay, despite being less sensitive and quantitative, revealed that the mutant lines, excluding R109A, demonstrated intermediate levels of NAD(P)H, indicating only partial correction of the EM9 repair deficiency (Fig. 3B). The R109A mutant, on the other hand, behaved more like wild-type XRCC1 (EM9-WT).

SSBs and SSBR kinetics were next examined before and after MMS treatment using an alkaline comet assay. This method allows for the detection of strand breaks and alkali-labile sites in individual cells [Singh et al., 1988]. Our studies of the various EM9 cell lines revealed that without MMS treatment the basal levels of DNA damage were inversely related to the complementation efficiency (see Fig. 3A) of the given XRCC1 protein: i.e., V86R (highest damage, lowest efficiency) > E69K > F67A ≥ WT ≅ R109A (lowest damage, highest efficiency) (Fig. 4A). Similarly, the level of SSBs in EM9-WT immediately after MMS treatment (0 min) was lower than in the EM9-V or EM9 mutant-complemented lines, although least so for R109A (Fig. 4A). At 30 min post-MMS treatment, the total damage actually increased in all cell lines, likely reflecting production of BER intermediates (alkali-sensitive AP sites or

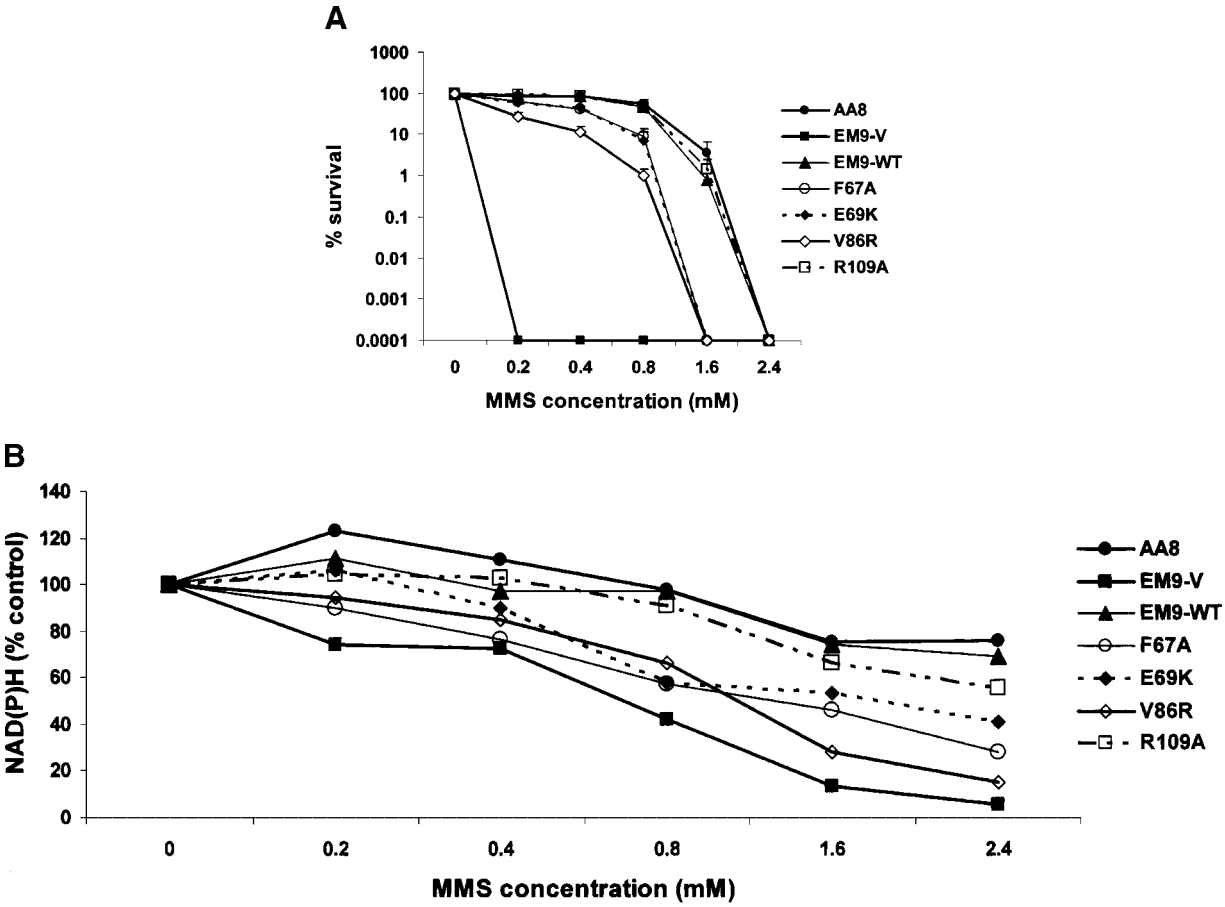

Fig. 3. Effect of site-specific mutations in NTD on MMS resistance. **A**: Complementation by various XRCC1 proteins. The cells lines indicated were exposed to MMS at different concentrations (denoted) for 1 h and incubated for 7–10 days in drug-free medium (see ''Materials and Methods'' for details). The surviving fraction of cells (percentage survival) was calculated by dividing the number of colonies in treated dishes by those counted in the untreated control. Values are the mean and standard deviation of at least three independent experiments. **B**: Single-strand break repair (SSBR) in the various cell lines as assessed by intracellular NAD(P)H levels. Cells were treated with MMS (concentrations indicated) for 1h, and the intracellular NAD(P)H level in living cells was determined as described in Materials and Methods. Shown is a representative experiment of three independent runs, plotting the NAD(P)H levels relative to 100% (i.e., percentage control).

SSBs) during the early stages of repair (only marginal repair was seen at 2 h as well, data not shown). Notably, this finding is similar to what was observed by Taylor et al. [2002], who reported an increase in alkali-labile sites at short time points following MMS treatment. After a 4 h incubation in drug free medium to permit recovery, the damage induced by MMS was found to be repaired most efficiently in EM9-WT and EM9 transfected with F67A, E69K, or R109A (Fig. 4). On the contrary, the tail moment of EM9 transfected with XRCC1 V86R was similar to the repair-defective EM9-V cells following the 4-h recovery. Thus, the V86R mutant, relative to the other site-specific mutants, exhibited the most pronounced (~twofold) and readily detectable reduction in SSBR kinetics (Fig. 4B). The apparent intermediate repair efficiency of R109A (Fig. 4B) stems largely from the lower levels of initial damage (which likely reflects repair during the MMS exposure), with the general pattern best mirroring EM9-WT (Fig. 4A).

DISCUSSION

XRCC1-deficient cell lines exhibit a defect in DNA repair, demonstrated as DNA-damaging agent hypersensitivity, reduced SSB processing, and markedly elevated SCEs [Thompson and West, 2000]. Since this protein has no known enzymatic activity, it has been proposed to function primarily as a scaffold protein in BER/SSBR processes, facilitating interactions

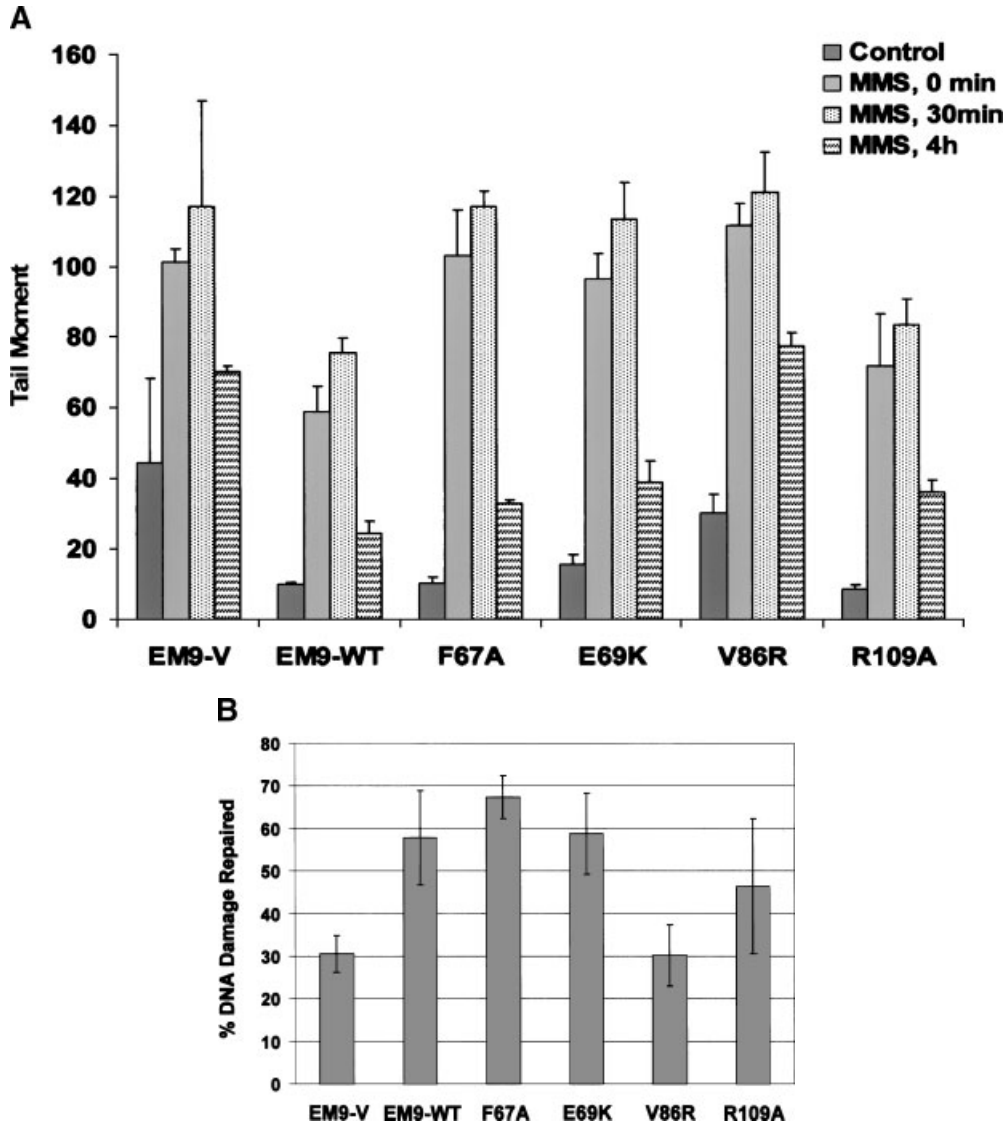

Fig. 4. SSBR proficiency in EM9 complemented cell lines. **A**: SSBR capacity in the various cell lines. DNA strand breaks (tail moment) was quantified in the indicated cells treated with either 0 (control) or 0.6 mM MMS for 10 min, followed by a 0, 30, or 240 min (4 h) incubation in drug-free medium to allow repair. Cells were subjected to the alkali comet assay as described in ''Materials and Methods''. Values are the mean and standard deviation of at least three independent experiments. **B**: DNA repair percentage after 240 min in drug-free medium. Data indicates the percentage of DNA damage repaired at 4 h relative to the MMS, 0 min time point. Values represent the average and estimated error as propogated from the numerator and denominator values of panel A.

between several key factors of these related pathways [Caldecott, 2003]. Reduced ligation activity in EM9 cell extracts was the first evidence for an in vivo role of XRCC1, later found to be the result of lower DNA Lig3α protein levels [Caldecott et al., 1995]. More recent site-specific mutant data showing that the BRCT-2 domain of XRCC1 (which directs a stabilizing interaction with Lig3α) is required for SSBR in G_1 offered additional support for the biological importance of the XRCC1–Lig3α interaction [Taylor et al., 1998, 2000]. PARP-1 has been shown to be critical for recruiting XRCC1 to sites of DNA damage, namely strand breaks, in both cellular localization (foci formation) and site-specific mutant studies [El Khamisy et al., 2003; Okano et al., 2003]. In addition, reduced SSB processing of 3′-phosphate residues by EM9 cell extracts suggests a physiological role for the XRCC1–PNK interaction [Whitehouse et al., 2001]. The recent finding that phosphorylation of XRCC1 by protein kinase CK2 affects

the in vivo co-localization of XRCC1 and PNK at the sites of DNA strand breakage further defends the biological importance of this association [Loizou et al., 2004]. While in vitro experiments have shown a tight association between XRCC1 and POLβ [Kubota et al., 1996; Marintchev et al., 2000], in vivo validation of the importance of this interaction has been lacking (see later). Likewise, biochemical studies have suggested a nick and gap-specific DNA binding activity for XRCC1 [Marintchev et al., 1999], although supporting cell biology data is presently absent.

To address issues related to the biological significance of specific XRCC1 functions, we generated four site-specific XRCC1 mutants and appropriate complemented EM9 cell lines (Fig. 2). We report here that each XRCC1 mutant defective in its ability to interact with POLβ (specifically, E69K and V86R; [Marintchev et al., 2003]) is incomplete at correcting the alkylation sensitivity of EM9 mutant cells (Fig. 3). The EM9-V86R line also exhibits a reduced rate of SSBR as determined by the comet assay (Fig. 4 and see further discussion below). These studies demonstrate the physiological importance of the XRCC1–POLβ interaction in facilitating efficient DNA repair responses.

Our data with the R109A XRCC1 mutant, engineered to be defective in DNA binding activity of XRCC1-NTD [Marintchev et al., 1999; 2003], suggests that this function is biologically less critical, at least in terms of the cellular end-points addressed here (i.e., alkylation sensitivity and SSBR kinetics). Consistent with this conclusion, the F67A mutant, defective in its ability to interact with both POLβ and substrate DNA [Marintchev et al., 1999, 2003], exhibited a complementation efficiency similar (but not additive) to the POLβ interaction mutants (E69K and V86R). Thus, the findings with the F67A mutant further support the biological importance of the POLβ interaction. The implication that the proposed N-terminal DNA binding function of XRCC1 is not essential is also consistent with the fact that we have been unable to reproduce the damage-specific DNA binding activity previously reported for the XRCC1-NTD [Marintchev et al., 1999] when using purified full-length recombinant human XRCC1 protein in vitro (Jinshui Fan and David Wilson, unpublished observations). While additional studies are underway to further interrogate possible DNA binding activities of XRCC1, the current data suggest that XRCC1 is directed to SSBs in vivo primarily via its interaction with PARP-1 and/or DNA Lig3α [El Khamisy et al., 2003; Leppard et al., 2003; Okano et al., 2003], or perhaps through its interaction with POLβ [Marintchev et al., 2003].

Some observations within warrant further discussion. First, POLβ levels, unlike Lig3α, appear to be largely unaffected by the presence or absence of XRCC1 (Fig. 2B, middle panel). This finding suggests that XRCC1 does not operate as a stabilizing factor for this protein in vivo, as it does with DNA Lig3α. Second, the E69K protein migrates more rapidly than the other XRCC1 proteins in SDS–polyacrylamide gels (Fig. 2B, top panel). While the reason for this mobility difference is unknown, we can exclude the possibility that errors in the DNA expression plasmid are responsible, as the pcDNA3-E69K template was confirmed by nucleotide sequencing. In addition, since this atypical migrating species was seen in eight independent cell lines stably-transfected with the pcDNA3-E69K vector, we can eliminate the possibility that the clonal EM9-E69K line used here was a unique and/or mutated isolate. Possible explanations for the altered mobility of the E69K protein includes defective post-translational modification, increased proteolytic susceptibility, or simply altered electrophoretic mobility properties. Significantly, XRCC1 has been found to be a substrate of protein kinases [Kubota and Horiuchi, 2003; Loizou et al., 2004], although, the E69 residue does not lie within a known phosphorylation site. Third, it is noteworthy that the XRCC1–POLβ-interaction mutants appreciably complement the EM9 repair defects (Fig. 3). These results indicate that (i) the physical association between XRCC1 and POLβ is only partly responsible for the deficiencies of XRCC1 mutant cells and (ii) other functions of XRCC1 (e.g., its interaction with PARP-1 and Lig3α) are accountable for the pronounced correction observed and are quantitatively more critical to the defects associated with EM9 mutant cells. Along these lines, it is noteworthy that the V86R mutant, which exhibited the worst complementation efficiency in terms of both MMS resistance and SSBR kinetics (Figs. 3 and 4), was least capable at restoring the Lig3 protein levels to normal (Fig. 2B, bottom panel). This observation implies that the poorer complementation seen

with V86R is the additive effect of multiple interaction defects and argues that the defective SSBR kinetics of XRCC1-deficient cells is mainly the product of reduced ligation capacity (Fig. 4), which is likely the rate-limiting step [Caldecott et al., 1994; Cappelli et al., 1997; Dianova et al., 2004].

We note that while preparing this manuscript, Dianova et al. [2004] reported that the V86R mutant is defective in its interaction with POLβ and unable to restore wild-type resistance to EMC11 XRCC1-mutant cells to hydrogen peroxide challenges. This finding extends our observations here—that the XRCC1-POLβ interaction is important for alkylation resistance and in SSBR—to indicate that the XRCC1–POLβ interaction is important in protecting against the cytotoxic effects of oxidative stress as well. Dianova et al., [2004] went on to show that the interaction of XRCC1 with POLβ operates to promote full ligation activity of the heterodimer complex XRCC1–Lig3α. Thus, the current picture suggests that XRCC1 is recruited to DNA strand breaks, presumably through its interaction with PARP-1, Lig3α, and/or POLβ, where its interaction with POLβ likely promotes SSB processing by activating the rate-limiting nick ligation activity of DNA Lig3α.

ACKNOWLEDGMENTS

We thank Dr. Alokes Majumdar, Sally Richards, Jeanine Harrigan, Jinshui Fan, and Mr. Al May (from the NIA) and Dr. Jean-Luc Ravanat from Laboratoire des acides Nucleiques (CEA, Grenoble, France) for assistance with technical and theoretical aspects of the science within. We also thank Dr. Nadja de Souza-Pinto, Dr. Michael Seidman, and Dr. Jeanine Harrigan for critical reading of and constructive input on the article.

REFERENCES

Barrows LR, Holden JA, Anderson M, D'Arpa P. 1998. The CHO XRCC1 mutant, EM9, deficient in DNA ligase III activity, exhibits hypersensitivity to camptothecin independent of DNA replication. Mutat Res 408:103–110.

Caldecott KW. 2003. XRCC1 and DNA strand break repair. DNA Repair (Amst) 2:955–969.

Caldecott KW, McKeown CK, Tucker JD, Ljungquist S, Thompson LH. 1994. An interaction between the mammalian DNA repair protein XRCC1 and DNA ligase III. Mol Cell Biol 14:68–76.

Caldecott KW, Tucker JD, Stanker LH, Thompson LH. 1995. Characterization of the XRCC1-DNA ligase III complex in vitro and its absence from mutant hamster cells. Nucleic Acids Res 23:4836–4843.

Cantoni O, Murray D, Meyn RE. 1987. Induction and repair of DNA single-strand breaks in EM9 mutant CHO cells treated with hydrogen peroxide. Chem Biol Interact 63:29–38.

Cappelli E, Taylor R, Cevasco M, Abbondandolo A, Caldecott K, Frosina G. 1997. Involvement of XRCC1 and DNA ligase III gene products in DNA base excision repair. J Biol Chem 272:23970–23975.

de Murcia G, Menissier dM. 1994. Poly(ADP-ribose) polymerase: A molecular nick-sensor. Trends Biochem Sci 19:172–176.

Demple B, DeMott MS. 2002. Dynamics and diversions in base excision DNA repair of oxidized abasic lesions. Oncogene 21:8926–8934.

Dianova II, Sleeth KM, Allinson SL, Parsons JL, Breslin C, Caldecott KW, Dianov GL. 2004. XRCC1-DNA polymerase beta interaction is required for efficient base excision repair. Nucleic Acids Res 32:2550–2555.

El Khamisy SF, Masutani M, Suzuki H, Caldecott KW. 2003. A requirement for PARP-1 for the assembly or stability of XRCC1 nuclear foci at sites of oxidative DNA damage. Nucleic Acids Res 31:5526–5533.

Fan J, Otterlei M, Wong HK, Tomkinson AE, Wilson DM, III. 2004. XRCC1 co-localizes and physically interacts with PCNA. Nucleic Acids Res 32:2193–2201.

Gryk MR, Marintchev A, Maciejewski MW, Robertson A, Wilson SH, Mullen GP. 2002. Mapping of the interaction interface of DNA polymerase beta with XRCC1. Structure (Camb) 10:1709–1720.

Gueven N, Becherel OJ, Kijas A, Chen P, Howe O, Rudolph JH, Gatti R, Date H, Onodera O, Taucher-Scholz G, Lavin MF. 2004. Aprataxin, a novel protein that protects against genotoxic stress. Hum Mol Genet 13:1081–1093.

Helleday T. 2003. Pathways for mitotic homologous recombination in mammalian cells. Mutat Res 532:103–115.

Hoy CA, Salazar EP, Thompson LH. 1984. Rapid detection of DNA-damaging agents using repair-deficient CHO cells. Mutat Res 130:321–332.

Kubota Y, Horiuchi S. 2003. Independent roles of XRCC1's two BRCT motifs in recovery from methylation damage. DNA Repair (Amst) 2:407–415.

Kubota Y, Nash RA, Klungland A, Schar P, Barnes DE, Lindahl T. 1996. Reconstitution of DNA base excision-repair with purified human proteins: Interaction between DNA polymerase beta and the XRCC1 protein. EMBO J 15:6662–6670.

Leppard JB, Dong Z, Mackey ZB, Tomkinson AE. 2003. Physical and functional interaction between DNA ligase IIIalpha and poly(ADP-Ribose) polymerase 1 in DNA single-strand break repair. Mol Cell Biol 23:5919–5927.

Lindahl T. 1993. Instability and decay of the primary structure of DNA. Nature 362:709–715.

Lindahl T, Satoh MS, Poirier GG, Klungland A. 1995. Post-translational modification of poly(ADP-ribose) polymerase induced by DNA strand breaks. Trends Biochem Sci 20:405–411.

Ljungquist S, Kenne K, Olsson L, Sandstrom M. 1994. Altered DNA ligase III activity in the CHO EM9 mutant. Mutat Res 314:177–186.

Loizou JI, El Khamisy SF, Zlatanou A, Moore DJ, Chan DW, Qin J, Sarno S, Meggio F, Pinna LA, Caldecott KW.

2004. The protein kinase CK2 facilitates repair of chromosomal DNA single-strand breaks. Cell 117:17–28.
Marintchev A, Mullen MA, Maciejewski MW, Pan B, Gryk MR, Mullen GP. 1999. Solution structure of the single-strand break repair protein XRCC1 N-terminal domain. Nat Struct Biol 6:884–893.
Marintchev A, Robertson A, Dimitriadis EK, Prasad R, Wilson SH, Mullen GP. 2000. Domain specific interaction in the XRCC1-DNA polymerase beta complex. Nucleic Acids Res 28:2049–2059.
Marintchev A, Gryk MR, Mullen GP. 2003. Site-directed mutagenesis analysis of the structural interaction of the single-strand-break repair protein, X-ray cross-complementing group 1, with DNA polymerase beta. Nucleic Acids Res 31:580–588.
Marsin S, Vidal AE, Sossou M, Menissier-de Murcia J, Le Page F, Boiteux S, de Murcia G, Radicella JP. 2003. Role of XRCC1 in the coordination and stimulation of oxidative DNA damage repair initiated by the DNA glycosylase hOGG1. J Biol Chem 278:44068–44074.
Masson M, Niedergang C, Schreiber V, Muller S, Menissier-de Murcia J, de Murcia G. 1998. XRCC1 is specifically associated with poly(ADP-ribose) polymerase and negatively regulates its activity following DNA damage. Mol Cell Biol 18:3563–3571.
Moore DJ, Taylor RM, Clements P, Caldecott KW. 2000. Mutation of a BRCT domain selectively disrupts DNA single-strand break repair in noncycling Chinese hamster ovary cells. Proc Natl Acad Sci USA 97:13649–13654.
Nakamura J, Asakura S, Hester SD, de Murcia G, Caldecott KW, Swenberg JA. 2003. Quantitation of intracellular NAD(P)H can monitor an imbalance of DNA single strand break repair in base excision repair deficient cells in real time. Nucleic Acids Res 31:e104.
Nash RA, Caldecott KW, Barnes DE, Lindahl T. 1997. XRCC1 protein interacts with one of two distinct forms of DNA ligase III. Biochemistry 36:5207–5211.
Nishino T, Morikawa K. 2002. Structure and function of nucleases in DNA repair: Shape, grip and blade of the DNA scissors. Oncogene 21:9022–9032.
Okano S, Lan L, Caldecott KW, Mori T, Yasui A. 2003. Spatial and temporal cellular responses to single-strand breaks in human cells. Mol Cell Biol 23:3974–3981.
Plo I, Liao ZY, Barcelo JM, Kohlhagen G, Caldecott KW, Weinfeld M, Pommier Y. 2003. Association of XRCC1 and tyrosyl DNA phosphodiesterase (Tdp1) for the repair of topoisomerase I-mediated DNA lesions. DNA Repair (Amst) 2:1087–1100.
Sano Y, Date H, Igarashi S, Onodera O, Oyake M, Takahashi T, Hayashi S, Morimatsu M, Takahashi H, Makifuchi T, Fukuhara N, Tsuji S. 2004. Aprataxin, the causative protein for EAOH is a nuclear protein with a potential role as a DNA repair protein. Ann.Neurol 55:241–249.
Schreiber V, Ame JC, Dolle P, Schultz I, Rinaldi B, Fraulob V, Menissier-de Murcia J, de Murcia G. 2002. Poly(ADP-ribose) polymerase-2 (PARP-2) is required for efficient base excision DNA repair in association with PARP-1 and XRCC1. J Biol Chem 277:23028–23036.
Shen MR, Zdzienicka MZ, Mohrenweiser H, Thompson LH, Thelen MP. 1998. Mutations in hamster single-strand break repair gene XRCC1 causing defective DNA repair. Nucleic Acids Res 26:1032–1037.
Singh NP, McCoy MT, Tice RR, Schneider EL. 1988. A simple technique for quantitation of low levels of DNA damage in individual cells. Exp Cell Res 175:184–191.
Speit G, Hartmann A. 1999. The comet assay (single-cell gel test). A sensitive genotoxicity test for the detection of DNA damage and repair. Methods Mol Biol 113:203–212.
Taylor RM, Wickstead B, Cronin S, Caldecott KW. 1998. Role of a BRCT domain in the interaction of DNA ligase III-alpha with the DNA repair protein XRCC1. Curr Biol 8:877–880.
Taylor RM, Moore DJ, Whitehouse J, Johnson P, Caldecott KW. 2000. A cell cycle-specific requirement for the XRCC1 BRCT II domain during mammalian DNA strand break repair. Mol Cell Biol 20:735–740.
Taylor RM, Thistlethwaite A, Caldecott KW. 2002. Central role for the XRCC1 BRCT I domain in mammalian DNA single-strand break repair. Mol Cell Biol 22:2556–2563.
Tebbs RS, Flannery ML, Meneses JJ, Hartmann A, Tucker JD, Thompson LH, Cleaver JE, Pedersen RA. 1999. Requirement for the Xrcc1 DNA base excision repair gene during early mouse development. Dev Biol 208:513–529.
Thompson LH, West MG. 2000. XRCC1 keeps DNA from getting stranded. Mutat Res 459:1–18.
Thompson LH, Brookman KW, Dillehay LE, Carrano AV, Mazrimas JA, Mooney CL, Minkler JL. 1982. A CHO-cell strain having hypersensitivity to mutagens, a defect in DNA strand-break repair, and an extraordinary baseline frequency of sister-chromatid exchange. Mutat Res 95:427–440.
Thompson LH, Brookman KW, Jones NJ, Allen SA, Carrano AV. 1990. Molecular cloning of the human XRCC1 gene, which corrects defective DNA strand break repair and sister chromatid exchange. Mol Cell Biol 10:6160–6171.
Vidal AE, Boiteux S, Hickson ID, Radicella JP. 2001. XRCC1 coordinates the initial and late stages of DNA abasic site repair through protein-protein interactions. EMBO J 20:6530–6539.
Whitehouse CJ, Taylor RM, Thistlethwaite A, Zhang H, Karimi-Busheri F, Lasko DD, Weinfeld M, Caldecott KW. 2001. XRCC1 stimulates human polynucleotide kinase activity at damaged DNA termini and accelerates DNA single-strand break repair. Cell 104:107–117.
Wilson SH. 1998. Mammalian base excision repair and DNA polymerase beta. Mutat Res 407:203–215.
Wilson DM, III, Sofinowski TM, McNeill DR. 2003. Repair mechanisms for oxidative DNA damage. Front Biosci 8:d963–d981.